Biochemistry

Article

Cite This: *Biochemistry* 2018, 57, 5513−5523

pubs.acs.org/biochemistry

Analysis of the Active Site Cysteine Residue of the Sacrificial Sulfur Insertase LarE from *Lactobacillus plantarum*

Matthias Fellner,[†,⊥] Joel A. Rankin,[†] Benoît Desguin,[‡] Jian Hu,[†,§] and Robert P. Hausinger*[,†,∥]

[†]Department of Biochemistry and Molecular Biology, Michigan State University, East Lansing, Michigan 48824, United States

[‡]Institute of Life Sciences, Université catholique de Louvain, B-1348 Louvain-La-Neuve, Belgium

[§]Department of Chemistry, Michigan State University, East Lansing, Michigan 48824, United States

[∥]Department of Microbiology and Molecular Genetics, Michigan State University, East Lansing, Michigan 48824, United States

Supporting Information

ABSTRACT: LarE from *Lactobacillus plantarum* is an ATP-dependent sulfur transferase that sacrifices its Cys176 sulfur atom to form a dehydroalanine (Dha) side chain during biosynthesis of the covalently linked nickel-pincer nucleotide (NPN) cofactor (pyridinium 3-thioamide-5-thiocarboxylic acid mononucleotide) of lactate racemase. Coenzyme A (CoA) stabilizes LarE and forms a CoA-Cys176 mixed disulfide with the protein. This study presents the crystal structure of the LarE/CoA complex, revealing protein interactions with CoA that mimic those for binding ATP. CoA weakly inhibits LarE activity, and the persulfide of CoA is capable of partially regenerating functional LarE from the Dha176 form of the protein. The physiological relevance of this cycling reaction is unclear. A new form of LarE was discovered, an NPN-LarE covalent adduct, explaining prior results in which activation of the lactate racemase apoprotein required only the isolated LarE. The crystal structure of the inactive C176A variant revealed a fold essentially identical to that of wild-type LarE. Additional active site variants of LarE were created and their activities characterized, with all LarE variants analyzed in terms of the structure. Finally, the *L. plantarum* LarE structure was compared to a homology model of *Thermoanaerobacterium thermosaccharolyticum* LarE, predicted to contain three cysteine residues at the active site, and to other proteins with a similar fold and multiple active site cysteine residues. These findings suggest that some LarE orthologs may not be sacrificial but instead may catalyze sulfur transfer by using a persulfide mechanism or from a labile site on a [4Fe-4S] cluster at this position.

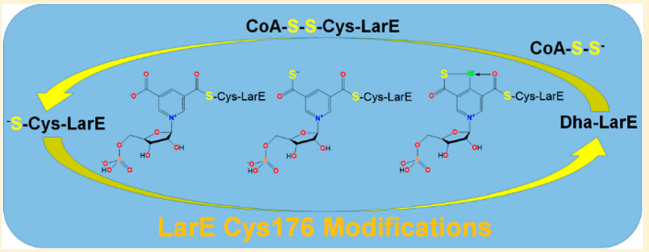

Lactate racemase (Lar) interconverts the D and L isomers of lactic acid, a central metabolite of many microorganisms.[1] The enzyme allows for the production of D-lactate for cell wall biosynthesis in bacteria that possess only L-lactate dehydrogenase and permits the metabolism of both isomers from racemic mixtures of lactate in microorganisms containing a single form of lactate dehydrogenase.[2−4] The Lar enzyme from *Lactobacillus plantarum* includes the protein LarA (UnitProtKB entry F9USS9) and a covalently tethered (via Lys184) cofactor, pyridinium 3-thioamide-5-thiocarboxylic acid mononucleotide with nickel bound to C4 of the pyridinium ring, the two sulfur atoms of the pincer complex, and the His200 side chain (Figure 1).[5,6] This organometallic complex will subsequently be termed the nickel-pincer nucleotide (NPN) cofactor.[7] The NPN cofactor is synthesized from nicotinic acid adenine dinucleotide (NaAD) by the sequential actions of LarB (UniProtKB entry F9UST0),[8] which carboxylates C5 of the pyridinium ring and hydrolyzes the phosphoanhydride bond, LarE (UniProtKB entry F9UST4), which converts the two carboxylates to thiocarboxylates,[9] and LarC (UniProtKB entry F9UST1), which installs the nickel.[8,10] The process by which the NPN cofactor becomes covalently attached to LarA from *L. plantarum* has not been described, and activation of LarA from *Thermoanaerobacterium thermosaccharolyticum* (UniProtKB entry D9TQ02) does not require adduct formation.[8]

This study focuses on LarE, a member of the PP-loop pyrophosphatase family containing a PP-loop SGGxDS motif in its N-terminal region. Transformation of pyridinium 3,5-biscarboxylic acid mononucleotide (P2CMN) to pyridinium 3,5-bisthiocarboxylic acid mononucleotide (P2TMN) by LarE requires two cycles of carboxylate activation (involving ATP-dependent adenylylation) and sulfur insertion, with the sulfur originating from a cysteine residue (Cys176) of the protein, thus making LarE a sacrificial sulfur transferase that acquires a dehydroalanine (Dha) residue.[8,9]

Here, we examine several unusual and interesting features of LarE with focus on its Cys176 residue. First, we investigate the unresolved nonsubstrate interaction of LarE with coenzyme A (CoA), a cellular component that stabilizes LarE and forms a disulfide with Cys176 but is not believed to be required for LarE activity,[8,9] by presenting the crystal structure of LarE with

Received: May 29, 2018
Revised: August 28, 2018
Published: August 29, 2018

DOI: 10.1021/acs.biochem.8b00601
Biochemistry 2018, 57, 5513−5523

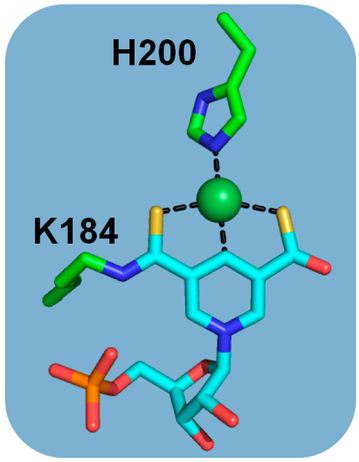

Figure 1. NPN cofactor in lactate racemase. Lys184 of LarA binds pyridinium 3-thioamide-5-thiocarboxylic acid mononucleotide [shown as sticks with cyan carbon atoms; Protein Data Bank (PDB) entry 5HUQ]. Two sulfur atoms and one carbon atom of the cofactor along with His200 coordinate nickel (green sphere).

bound CoA. Second, we provide evidence that CoA weakly inhibits LarE activity. Third, we demonstrate the ability of CoA-persulfide to regenerate Cys-containing LarE from the Dha176-containing protein ($LarE^{Dha}$). Fourth, we provide evidence of the presence of a novel NPN adduct of LarE, providing an explanation for earlier confounding observations related to the ability of purified LarE to activate the LarA apoprotein. Fifth, we investigate whether the loss of the Cys176 side chain significantly impacts the protein fold by characterizing the structure of the C176A variant. Sixth, we characterize the functions of several other key residues of LarE and summarize all LarE mutagenesis studies to better define the sacrificial sulfur insertion reaction.[9] Lastly, we speculate about whether LarE homologues containing additional active site cysteine residues may operate by a catalytic sulfur transfer process.

MATERIALS AND METHODS

Genes, Plasmids, and Cloning. Site-directed mutagenesis of the gene encoding Strep II-tagged wild-type (WT) LarE from *L. plantarum* was performed using a QuikChange mutagenesis kit (Agilent) for creating the K101A, E128A, and E223A variants. All of the constructs were verified by DNA sequencing. Details, including instructions for creating the C176A variant, are summarized in our previous work.[9]

LarE Overexpression, Purification, and Characterization. WT, C176A, and the new variant forms of LarE were overexpressed and purified using our previously described pGIR076 *Escherichia coli* ArcticExpress-Strep-tactin (IBA) system.[9] The final buffer for all samples was 100 mM Tris-HCl (pH 7.5) containing 300 mM NaCl. The activities of WT and variant forms of LarE were assessed by monitoring samples for their abilities to transform P2CMN to P2TMN that was further metabolized by LarC and incorporated into LarA apoprotein from *T. thermosaccharolyticum*; this activated LarA enzyme was then assayed for lactate racemization as described elsewhere in detail.[9]

Crystallization. For both the CoA-bound WT protein and the C176A LarE variant, crystals were obtained after mixing 5 μL of protein samples with 5 μL of reservoir solutions. The hanging drop reservoir contained 100 μL of 30.0% (v/v) pentaerythritol ethoxylate (15/4 EO/OH), 50 mM Bis-Tris (pH 6.5), and 100 mM ammonium sulfate. The CoA-bound sample contained 28 mg/mL WT LarE mixed with 0.9 mM CoA and was incubated for ∼10 min on ice before setting up the drop. The C176A LarE sample contained 8 mg/mL variant protein. Using the same setup that was used for C176A, we also set up unsuccessful crystal drops for W97A (∼1 mg/mL), S180A (∼10, 12, and 15 mg/mL), R212A (∼6 mg/mL), and D231R (∼3, 11, and 24 mg/mL) variants of LarE using the same procedures.[9]

Diffraction Data Collection, Structure Determination, and Analysis. Data sets were collected at the Advanced Photon Source LS-CAT beamlines (21-ID-F and 21-ID-G). Data sets were processed with xdsapp[11] and iMos,[12] with merging and scaling done using aimless.[13] Phaser molecular replacement[14] was utilized using the WT apoprotein model 5UDQ. Model building and refinement were conducted in Coot[15] and Phenix.[14] Data set statistics are listed in Table 1. UCSF Chimera[16] was used to create structure figures.

Purification of Dha-Containing LarE. $LarE^{Dha}$ was purified from *Lactococcus lactis* NZ3900 containing pGIR172 that carries the *larA*−*larE* genes from *L. plantarum* with *larE* translationally fused to DNA encoding the Strep-tag II[5] as previously described.[8] The cells were grown overnight without being shaken in 15 mL of M17 medium (Oxoid or Difco) containing 0.5% (w/v) D-glucose and 10 mg/L chloramphenicol at 30 °C. This inoculum was added to 1.5 L of the same medium, but containing 5 mg/L chloramphenicol, and incubated at 28 °C while being shaken (40 rpm) until the OD_{600} reached ∼0.3. The culture was supplemented with 1 mM $NiCl_2$, induced with 10 μg/L nisin A (Sigma), and grown for 4 h before the cells were harvested by centrifugation at 5000*g* for 10 min. The cell pellet was washed using 100 mM Tris-HCl buffer (pH 7.5) containing 300 mM NaCl and stored until it was needed at −80 °C. The thawed cells were suspended in 40 mL of 100 mM Tris-HCl buffer (pH 7.5) containing 300 mM NaCl, 1 mM phenylmethanesulfonyl fluoride (PMSF, added as a 100 mM stock in ethanol), and 1 unit/mL Benzonase (Millipore) on ice and then lysed by two passes through a chilled French pressure cell at 16000 psi. The debris and intact cells were removed by centrifugation at 27000*g* and 4 °C for 40 min. Purification of $LarE^{Dha}$ was performed by using a 1 mL bed volume of Strep-tactin-XT (IBA) resin equilibrated in 20 mM Tris-HCl buffer (pH 7.5) containing 300 mM NaCl at 4 °C. The lysates were loaded at a rate of 1 mL/min; the resin was washed by gravity flow with five 1 mL additions of 20 mM Tris-HCl buffer (pH 7.5) containing 300 mM NaCl, and the protein was eluted with six 0.5 mL additions of 20 mM Tris-HCl buffer (pH 7.5) containing 300 mM NaCl and 50 mM biotin (Santa Cruz Biotechnology) that had been neutralized with 50 mM NaOH.

Additional characterization of $LarE^{Dha}$ included analysis of its reactivity with 5,5′-dithiobis(2-nitrobenzoic acid) (DTNB) and tris(2-carboxyethyl)phosphine (TCEP) in comparison to that of LarE. To quantify accessible thiol groups, the protein samples were treated with 180 μM DTNB in 100 mM Tris-HCl (pH 7.5), allowed to react for 30 min, and monitored at 412 nm.[17] For testing the reactivity of LarE-associated Dha with TCEP,[18] the samples were treated with 5 mM TCEP in buffer and analyzed by mass spectrometry (see below).

LarE Regeneration Reactions. Lysates for use in LarE regeneration experiments were derived from cultures of *L. plantarum* NCIMB8826. Using a 2% inoculum, the cells were

DOI: 10.1021/acs.biochem.8b00601
Biochemistry 2018, 57, 5513−5523

Table 1. Crystallography statistics for the CoA-Bound and C176A Variant LarE Structures

	CoA-bound	C176A
Data Collection[a]		
beamline	LS-CAT 21-ID-F	LS-CAT 21-ID-G
wavelength (Å)	0.979	0.979
space group	$P4_122$	$P4_122$
unit cell dimensions		
a, *b*, *c* (Å)	107, 107, 320	109, 109, 329
α, *β*, *γ* (deg)	90, 90, 90	90, 90, 90
resolution (Å)	47.95−2.09 (2.12−2.09)	48.67−2.35 (2.39−2.35)
no. of unique reflections	111492 (5293)	82741 (4345)
redundancy	6.1 (6.0)	11.3 (11.2)
completeness (%)	99.7 (97.1)	99.5 (97.3)
$I/\sigma I$	14.7 (1.8)	18.9 (2.1)
R_{merge}[b]	0.084 (0.899)	0.102 (1.079)
R_{pim}[c]	0.055 (0.599)	0.046 (0.482)
$CC_{1/2}$[d]	0.998 (0.509)	0.999 (0.702)
Refinement		
no. of protein atoms	11949	11420
no. of CoA atoms	288	0
no. of phosphate atoms	30	30
no. of sulfate atoms	0	25
no. of waters	606	493
R_{work}/R_{free}[e]	0.195/0.234	0.187/0.244
B factor (Å^2)	43.8	56.3
protein	43.9	57.0
CoA	59.5	–
phosphate	38.5	47.7
sulfate	–	61.5
water	42.5	48.4
root-mean-square deviation in bond lengths (Å)	0.007	0.007
root-mean-square deviation in bond angles (deg)	0.975	0.922
Ramachandran plot, favored (%)	97.34	97.43
Ramachandran plot, outliers (%)	0	0
no. of rotamer outliers	0	0
PDB entry	6B2M	6B2O

[a]Data for the highest-resolution shell are shown in parentheses. [b]$R_{merge} = \sum_{hkl}\sum_j|I_j(hkl) - \langle I(hkl)\rangle|/\sum_{hkl}\sum_j I_j(hkl)$, where *I* is the intensity of reflection. [c]$R_{pim} = \sum_{hkl}[1/(N-1)]^{1/2}\sum_j|I_j(hkl) - \langle I(hkl)\rangle|/\sum_{hkl}\sum_j I_j(hkl)$, where *N* is the redundancy of the data set. [d]$CC_{1/2}$ is the correlation coefficient of the half-data sets. [e]$R_{work} = \sum_{hkl}||F_{obs}| - |F_{calc}||/\sum_{hkl}|F_{obs}|$, where F_{obs} and F_{calc} are the observed and calculated structure factors, respectively. R_{free} is the cross-validation *R* factor for the test set of reflections (5% of the total) omitted during model refinement.

grown without being shaken at 37 °C in MRS medium (Sigma) supplemented with 0.1% (v/v) Tween 20. At an OD_{600} of ∼1, the cultures were induced by adding 200 mM sodium L-lactate as a dry powder or left uninduced and incubated for a further 2 h. The cells were harvested by centrifugation at 5000*g*, and the pellets were washed in 100 mM Tris-HCl buffer (pH 7.5) containing 150 mM NaCl and stored at −80 °C. The cells (∼500 μL of cell paste) were mixed with glass beads (∼500 μL, mean diameter of 100 μm) in 20 mM Tris-HCl (pH 7.5) containing 150 mM NaCl and, for maintaining anaerobic conditions,[19] 20 μg/mL glucose oxidase, 2 μg/mL catalase, and 0.3% (w/v) D-glucose in 1.5 mL screw cap tubes (deaerated by blowing argon over the surface) and lysed by using a Mini-Bead Beater 16 (BioSpec) with two 60 s pulses separated by 5 min on ice. The debris was removed by centrifugation at 20000*g* and 4 °C for 10 min.

Cysteine desulfurase (IscS) was purified from *E. coli* BL21 (DE3) containing pBH402, a plasmid with *E. coli iscS* fused to a sequence encoding a His_6 tag and under the control of the T7 promoter.[20] Overnight cultures of these cells were grown while being shaken (300 rpm) at 37 °C in LB containing 50 μg/mL kanamycin (Gold Biotechnology), then diluted 200-fold into 0.5 L of Lennox LB supplemented with 1 mM pyridoxine (Sigma) and 50 μg/mL kanamycin, and further grown while being shaken at the same temperature. When an OD_{600} of ∼0.5 was reached, the cultures were amended with 0.4 mM isopropyl β-D-1-thiogalactopyranoside and grown for an additional 3 h. The cells were collected by centrifugation and resuspended in 40 mL of buffer A [50 mM Na_2HPO_4 (pH 8.0) containing 300 mM NaCl and 20 mM imidazole] supplemented with 2.5 units/mL Benzonase and 1 mM PMSF. The suspension was chilled on ice and lysed by two passes through a chilled French press cell at 16000 psi. The cell debris was pelleted by centrifugation at 27000*g* and 4 °C for 40 min. The supernatant was applied to a column (10 mL) of Ni-nitrilotriacetic acid-Sepharose that had been equilibrated in buffer A. After the column had been washed twice with 50 mL of buffer A, IscS was eluted at a rate of 2 mL/min with a 100 mL linear gradient from buffer A to buffer A containing 500 mM imidazole. The 2.5 mL fractions were collected into tubes containing 2.5 μL of 10 mM EDTA (pH 8.0) to prevent precipitation. The IscS-containing fractions were combined and dialyzed overnight at 4 °C against 2 L of 50 mM potassium phosphate buffer (pH 7.5) containing 5 mM $MgCl_2$, 100 mM KCl, and 0.1 mM EDTA. The protein concentration was quantified using the published ε_{280} of 25400 M^{-1} cm^{-1},[20] and purified IscS was stored at 4 °C.

Organic persulfides were synthesized by incubating 5−20 mM disulfides with a 5-fold molar excess of NaHS in 300 mM Tris-HCl (pH 7.5, for making CoA and glutathione persulfides) or 100 mM NaOH (for the Cys persulfide) in an argon atmosphere.[21] The reaction mixtures were incubated at 30 °C for 30 min. Persulfide yields were quantified by using a cold cyanolysis procedure,[22] with yields typically of ∼30% relative to the starting disulfide concentrations. Persulfide preparations were used immediately without further purification or frozen at −20 °C under argon for later use.

$LarE^{Dha}$ (2.8 μM, 0.087 mg/mL) was incubated in 20 mM Tris-HCl buffer (pH 7.5) containing 150 mM NaCl, 20 μg/mL glucose oxidase, 2 μg/mL catalase, and 0.3% (w/v) D-glucose (to ensure anoxic conditions), with various additives as specified. Selected mixtures included 10% cell-free lysates from *L. plantarum* cultures that were induced with lactic acid or non-induced. Some mixtures included 2 mM $MgCl_2$ and 1 mM ATP. Individual sulfur sources and a combined mixture of sulfur compounds (1 mM cysteine, 1 mM glutathione, 1 mM 3-mercaptopyruvate, 1 mM sodium thiosulfate, 1 mM sodium sulfide, and 200 μM CoA) were tested. In addition, IscS (4.6 μM, 0.21 mg/mL) with 1 mM cysteine was examined. For all samples, the reaction mixtures were layered with mineral oil and allowed to incubate at room temperature with 1 mL time points taken at 1 h or overnight. The samples lacking cell-free lysates were directly analyzed by mass spectrometry, but those amended with lysates were loaded by gravity flow at 4 °C onto columns containing 200 μL of Strep-tactin-XT resin; the columns were washed using three 1 mL additions of 20 mM Tris-HCl buffer (pH 7.5) containing 150 mM NaCl, and the

DOI: 10.1021/acs.biochem.8b00601
Biochemistry 2018, 57, 5513−5523

LarE protein was eluted using six 250 μL additions of the same buffer containing 50 mM biotin neutralized with 50 mM NaOH. These protein samples were concentrated to at least 1 μM LarE using 10 kDa cutoff Amicon centrifuge columns prior to further analysis.

Mass Spectrometry of LarE. The purified LarE protein samples (10 μL in buffer), including those from the LarE regeneration studies, were injected onto a cyano-chemistry high-performance liquid chromatography column that was equilibrated in 0.1% formic acid and eluted with an increasing gradient of acetonitrile. The fractions were analyzed by electrospray ionization mass spectrometry (ESI-MS) using a XEVO G2-XS instrument in positive ionization mode. The protein masses were derived from the MS data using MaxEnt (Waters Corp.). LarE samples were also purified from *Lc. lactis* NZ3900 pGIR172 that had been induced for different lengths of time (1, 2, 3, and 4 h) and analyzed by the same ESI-MS approach.

LarE Enzyme Assay. The activity of LarE was assessed indirectly by a four-step process using purified components and assaying for Lar activity. The first step was the production of P2CMN by a 3 h incubation of LarB (3 μM) with 1 mM NaAD in 100 mM $NaHCO_3$ with quenching by heat (80 °C for 5 min). The second step involved LarE synthesis of P2TCM; the step 1 mixture (4% of the final volume) was incubated with 10 μM LarE, 2 mM reducing agent [Cys, dithiothreitol (DTT), CoA, β-mercaptoethanol, glutathione, or ascorbic acid], 2 mM ATP, and 20 mM $MgCl_2$ in 100 mM Tris-HCl (pH 7) for 5 min at room temperature, and then the reaction was stopped by heat. Step 3 involved synthesis of the NPN cofactor and generation of active LarA by reacting the step 2 mixture (10% of the final volume) with 1.5 μM LarC, 1.5 μM *T. thermosaccharolyticum* LarA apoprotein, 1 mM $MnCl_2$, 0.1 mM CTP, and 40 mM D-lactate in 100 mM Tris-HCl (pH 7) for 5 min at room temperature, with quenching by heat. The final step was to measure L-lactate with an enzymatic kit (Megazyme).

RESULTS

Structural Investigation of Cys176/Coenzyme A Interaction. Prior studies had demonstrated that the addition of CoA stimulates the activation of LarA apoprotein in mixtures containing P2CMN (the product of LarB), Mg·ATP, LarE, LarC, and LarA apoprotein.[8] Unpublished observations showed a 765 Da adduct present in LarE purified from *Lc. lactis* cells, which we presumed to be CoA. When LarE (as the Strep II-tagged species lacking the N-terminal Met residue; 31550 Da) was purified in the presence of CoA, this adduct (32316 Da) became the majority species and CoA was shown to form a disulfide with the single cysteine residue of LarE (Cys176).[8] Several thiol reductants (sulfide, Cys, DTT, and glutathione), including CoA, could reduce the disulfide and confer LarE activity in the Lar assay, but only CoA provided longer-term (20 h) stability to the protein (data not shown). An analogous CoA-protein disulfide (32274 Da) was formed with the D30A variant of LarE (31508 Da) but not with the C176A variant (31520 Da) (Figure 2). CoA is not required for *E. coli*-derived LarE to convert P2CMN to P2TMN.[9] The CoA-protein disulfide form of LarE converts to $LarE^{Dha}$ in the LarA apoprotein activation mixture. While it is clear that CoA interacts with LarE, further studies were required to establish the details of this interaction.

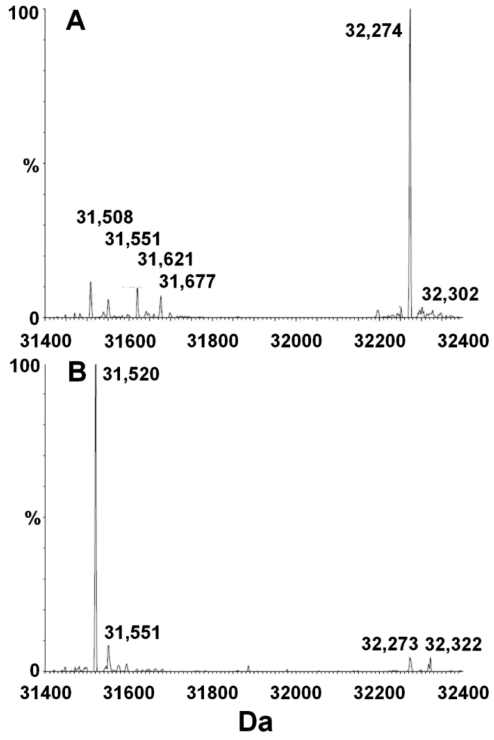

Figure 2. ESI-MS of (A) the CoA−S−S−Cys176 disulfide using D30A LarE and (B) the C176A variant of LarE, both purified in the presence of CoA.

LarE was isolated from both *Lc. lactis* and *E. coli* using purification buffers containing CoA, and each protein was crystallographically characterized. All LarE chains of the crystallographic hexamers had CoA bound. The phosphate group of the 3′-phosphoadenosine portion of the molecule was found at the PP loop (the ATP binding site) of LarE (Figure 3A). The adenine moiety forms two hydrogen bonds with the backbone atoms of Ala52 on strand β2. The ribose is stabilized via interactions with the backbone atoms of Ala24 on β1 and Gly123 on β4. The diphosphate group of CoA was well-ordered in all structures but exhibited slightly different orientations between chain C and all other chains (Figure 3B). The differences were more notable for the remaining pantoic acid-alanine-cystamine portions of CoA; this part of the molecule is less ordered in all chains, does not show direct contacts with the protein, and shows slight variations in chains A, B, and D−F (F is shown as a representative example) compared to the very different orientation in chain C (Figure 3B). The distinct orientations of the coenzyme paralleled the differences in side chain orientations of the key residue, Trp97.[9] Although MS experiments had previously indicated a disulfide bond between CoA and Cys176 of LarE,[8] no disulfide bond was detected in the electron density maps. This result suggested that photoreduction of the disulfide may have occurred during data collection. Notably, the CoA sulfur atom was in the vicinity of the Cys176 side chain, with the two different orientations having distances of 8.8 and 10.4 Å between the Cys176 and the CoA sulfur atoms. The transition between the two orientations of the least ordered portion of CoA would place the CoA sulfur close enough to the Cys176 side chain to form the disulfide.

The binding mode of the 3′-phosphoadenosine ribose portion of CoA is nearly identical to that of ATP, the

DOI: 10.1021/acs.biochem.8b00601
Biochemistry 2018, 57, 5513−5523

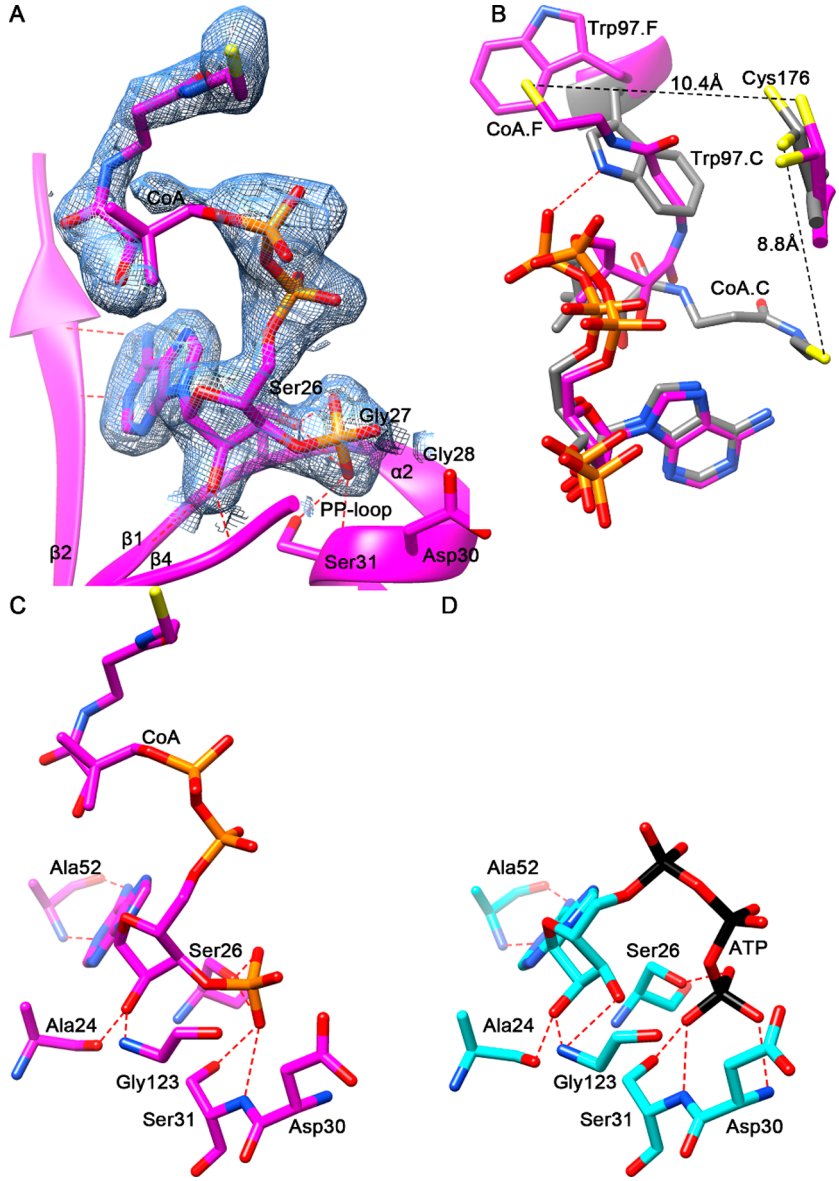

Figure 3. Binding of CoA to LarE (PDB entry 6B2M). All comparisons are based on a Cα alignment of the full length protein.[16] (A) The $2F_O - F_C$ map of CoA bound to chain F is shown as blue mesh at 1 σ. Interacting backbone residues are illustrated as ribbons with secondary structure features labeled, and the PP-loop residue side chains are shown. Hydrogen bonds are indicated as red dashes. (B) Comparison of CoA binding orientations in LarE. Chain F is colored magenta (representative for chains A, B, D, and E) and compared to chain C (gray). The corresponding side chains of Trp97 and Cys176 are illustrated in the same colors with distances between the CoA and Cys176 sulfur atoms shown as black dashes. (C and D) Comparison of CoA and ATP (PDB entry 5UDS)[9] binding to LarE. Interacting residues are shown in stick mode with hydrogen bonds indicated by red dashes. The carbon atoms of the CoA- and ATP-bound structures are colored magenta and cyan, respectively. The ligand phosphorus atoms of CoA are colored orange, and those of ATP are colored black.

difference being that the triphosphate of ATP is positioned to place the γ-phosphate into the PP loop, whereas it is the ribose phosphate group of CoA that is tightly associated with the PP-loop residues (Figure 3C,D).

CoA Weakly Inhibits LarE Activity. ATP likely has a binding affinity for LarE greater than that of CoA, compatible with its greater number of interactions involving the PP loop, thus overcoming any potent inhibitory effect of the coenzyme. Nevertheless, the apparent LarE activity was lower when using CoA compared to other reductants (Cys, DTT, β-mercaptoethanol, glutathione, or ascorbic acid) when the protein was subjected to short-term treatment with these reagents and analyzed using the indirect LarA apoprotein activation assay (Figure 4). This result suggests that CoA binding is partly inhibitory with respect to LarE activity.

Additional Characterization of LarE^{Dha}. Strep-tagged LarE was expressed in *Lc. lactis* in the context of the entire *lar* operon and purified. As previously described,[8] nearly all of the resulting LarE lacks its Cys176 sulfur atom according to ESI-MS (Figure 5A). This major form of the protein was observed for samples isolated from cultures that had been induced from 1 to 4 h (data not shown), so LarE^{Dha} is stable in the cells. Along with LarE^{Dha} (31517 Da) the spectrum reveals likely sodium complexes of the protein (≥31540 Da); the intensity of these forms was greatly reduced using an ammonium bicarbonate buffer. In contrast to the native LarE protein that exhibits DTNB reactivity accounting for 0.93 Cys thiol per

DOI: 10.1021/acs.biochem.8b00601
Biochemistry 2018, 57, 5513−5523

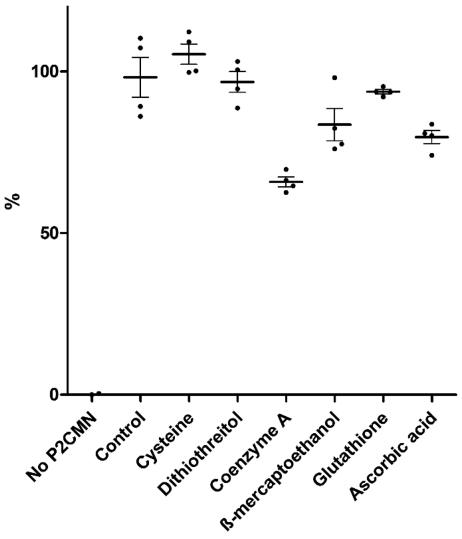

Figure 4. Inhibitory effect of CoA on the apparent LarE activity compared to other reductants. P2CMN was produced enzymatically from NaAD, converted to P2TMN by LarE in the presence of the indicated reductants (2 mM) along with 2 mM ATP and 20 mM $MgCl_2$ in 100 mM Tris-HCl buffer (pH 7), transformed into the NPN cofactor by LarC, incorporated into *T. thermosaccharolyticum* LarA apoprotein, and assayed for Lar activity, shown as the percent relative to the control without thiol.

protein, no 412 nm peak was detected in the $LarE^{Dha}$ protein. As further support for the presence of Dha, the addition of TCEP to $LarE^{Dha}$ led to partial modification to form a species at 31767 Da, or 250 Da larger than $LarE^{Dha}$ (Figure S1), consistent with the known reactivity of TCEP toward dehydroalanine,[18] whereas this reagent had no effect on the mass spectrum of LarE.

Regeneration of Cys-Containing LarE from $LarE^{Dha}$ by CoA Persulfide. Regeneration of native LarE from $LarE^{Dha}$ was achieved by using the persulfide of CoA followed by reduction with DTT (Scheme 1). Incubation of $LarE^{Dha}$ with CoA persulfide (Figure 5B) resulted in substantial conversion of the Dha-containing protein (31517 Da) to a species (32316 Da) consistent with the LarE−S−S−CoA disulfide. In addition, we noted a minor species (32285 Da) suggesting the formation of the LarE−S−CoA thioether. Consistent with the thioether interpretation, the same species formed for $LarE^{Dha}$ treated with CoA rather than the CoA persulfide (Figure S2). Subsequent reduction of the CoA persulfide mixture by DTT (Figure 5C) eliminated the putative disulfide species but not the proposed thioether and generated a peak (31551 Da) corresponding to native LarE. In contrast to the robust regeneration observed using the CoA persulfide, the Cys persulfide produced much lower levels of the LarE−S−S−Cys disulfide [31669 Da (Figure 5D)] and corresponding smaller amounts of the native LarE after reduction (Figure 5E). DTT reduction of the Cys persulfide-treated sample led to an increase in the 31669 Da species that we attribute to formation of the thioether between DTT and $LarE^{Dha}$, which happens to possess the same mass as the LarE−S−S−Cys disulfide, as confirmed by a control reaction of DTT and the Dha-containing protein (Figure S3). No reactivity was detected between the glutathione persulfide and $LarE^{Dha}$ (data not shown). These results suggest the CoA binding site of LarE is used to specifically bind the CoA persulfide during the sulfuration reaction. Although regeneration of

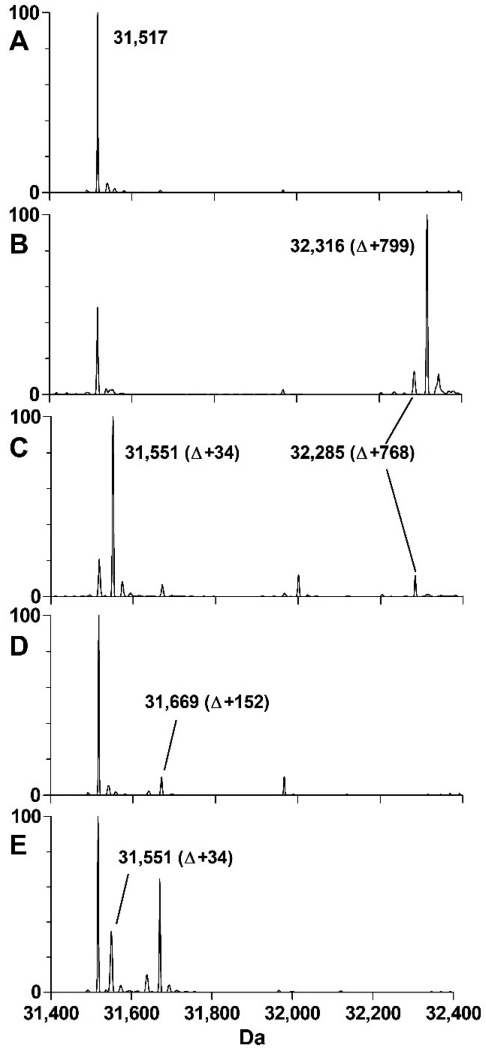

Figure 5. Regeneration of native LarE from $LarE^{Dha}$. (A) ESI-MS of $LarE^{Dha}$. (B) $LarE^{Dha}$ treated with CoA persulfide (150 μM, 1 h at room temperature and then overnight at 4 °C), revealing conversion to the LarE−S−S−CoA disulfide. (C) Sample from panel B reduced with DTT (10 mM, 30 min at room temperature) to generate native LarE. (D) $LarE^{Dha}$ treated with Cys persulfide. (E) Sample from panel D treated with DTT. The Δ values are relative to the 31517 Da value of $LarE^{Dha}$. The *y*-axes indicate the percent relative to the intensities of the maximum peaks.

Scheme 1

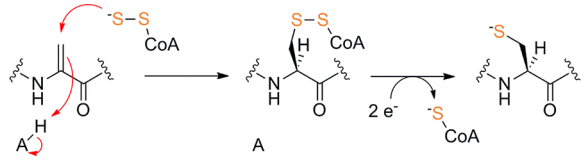

native LarE from $LarE^{Dha}$ was demonstrated by these *in vitro* experiments, it remains unclear whether a similar process occurs within *L. plantarum* cells.

Alternative efforts to reincorporate sulfur into the $LarE^{Dha}$ protein were unsuccessful. These included using a variety of *in vitro* conditions, a range of potential sulfur donors, lysates from native *L. plantarum* cells (induced by addition of L-lactate and non-induced controls), other potential cofactors ($MgCl_2$ and ATP, CoA, and glutathione), and cysteine and cysteine

DOI: 10.1021/acs.biochem.8b00601
Biochemistry 2018, 57, 5513−5523

desulfurase, a known sulfur source for several other biological sulfur-containing components. In none of these cases did we observe conversion of LarE^{Dha} to the WT species.

Discovery of an NPN Adduct of LarE^{Dha}. Some preparations of LarE^{Dha} possessed a previously undescribed species (31968 Da) that was 450 Da larger than the Dha-containing protein (31518 Da) (Figure 6). Interestingly, this

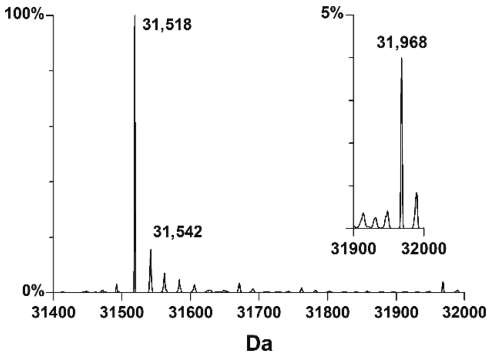

Figure 6. Example ESI-MS spectrum of LarE^{Dha} with an inset depicting an expanded view of the region from 31900 to 32000 Da.

species is consistent with the formation of a covalent adduct between NPN and LarE. Such a species explains a previous confounding observation related to LarA activation. Namely, the incubation of purified LarA (1.4 pmol) with LarE (280 pmol, isolated from cells containing LarB and LarC) was shown to result in activation of ~30% of the lactate racemase apoprotein.[5] We interpret this prior result as arising from a secondary pathway for LarA activation that utilizes this new species with NPN covalently attached to LarE.

Structural Characterization of C176A LarE and Functional Characterization of LarE Variants. We attempted to crystallize several LarE variants with largely reduced or abolished activity (W97A, C176A, S180A, and R212A) and the active D231R variant but had success only with the C176A LarE sample. The W97A variant, thought to be defective in its interaction with the P2CMN substrate,[9] was poorly produced, thus preventing crystallization. The S180A and R212A variants, considered to lack the P2CMN or inorganic phosphate binding site, were examined using many conditions, but the lack of successful crystallization suggests that a bound phosphate/sulfate molecule at this binding site is required for crystal formation. Although the D231R variant is as active as the WT enzyme, we observed no crystal formation, suggesting that the LarE trimer/hexamer interface where Asp231 is located may be disturbed, thus preventing crystal growth. The successful case of the C176A variant protein yielded the same crystal morphology and size as the WT enzyme.

The overall fold of the C176A LarE structure (Figure 7A) was identical to that of the WT protein. Even the flexible linker between domains on which Cys176 is located matched in both structures. In addition, the bound phosphate previously noted in the WT enzyme[9] was also present in the C176A structure, indicating that hydrogen bonding with the sulfur atom (Figure 7B) is not crucial for binding the phosphate of P2CMN. The loss of activity of the C176A variant must be based solely on the functional role of the thiol group as a sulfur donor as the C176A structure shows no other structural difference from the WT enzyme.

We previously characterized several LarE variants of highly conserved residues to show the importance of the active site cysteine (C176A), the PP loop (D30A), the P2CMN phosphate binding site (S180A and R212A), and several key residues in catalysis (W97A, R181K, and E200Q) while also ruling out the involvement of other residues (E61Q and D231R) (Figure 7B).[8,9] Here, we characterized three additional variants to gain an even better understanding of LarE's function. Glu223 is buried in a manner similar to that of Glu200 in the C-terminal head domain of LarE, which forms trimer/hexamer interactions and binds the phosphate moiety

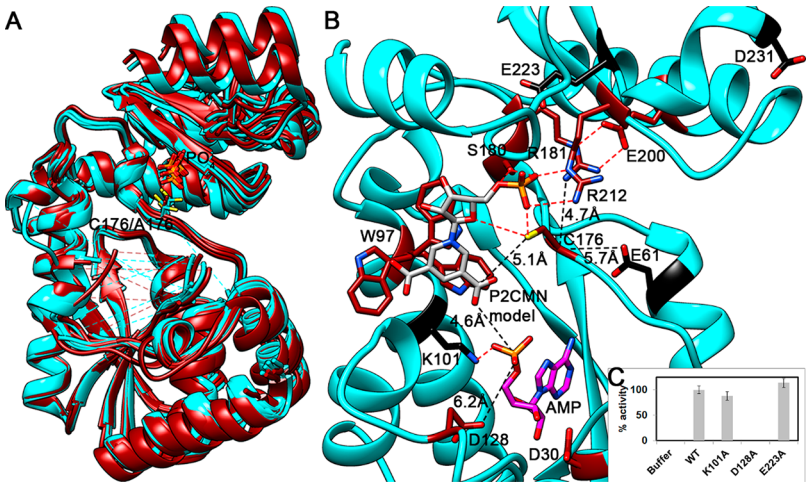

Figure 7. Analysis of LarE variants. (A) Comparison of the six chains of WT LarE colored cyan (PDB entry 5UDQ[9]) and those of the C176A LarE variant colored dark red (PDB entry 6B2O). The Cys176 side chain and nearby phosphate molecule are shown. (B) P2CMN/AMP-bound model of LarE based on chain A of NMN-bound LarE (PDB entry 5UDR) and chain C of AMP-bound LarE (PDB entry 5UDT).[9] Carbon atoms of the P2CMN model are colored gray, those of AMP magenta, and the side chains of residues that are altered in inactive variants dark red [D30A and C176A;[8] W97A, C176A, S180A, R181K, E200Q, and R212A;[9] and D128A (this publication)]. In addition, the side chains of residues that were substituted in active variants are colored black [E61Q and D231R[9] and K101A and E223A (this publication)]. Hydrogen bonds are shown as red dashes, and important interactions are illustrated as black dashes with the distances indicated. (C) Activity results of three variants characterized in this publication.

DOI: 10.1021/acs.biochem.8b00601
Biochemistry 2018, 57, 5513−5523

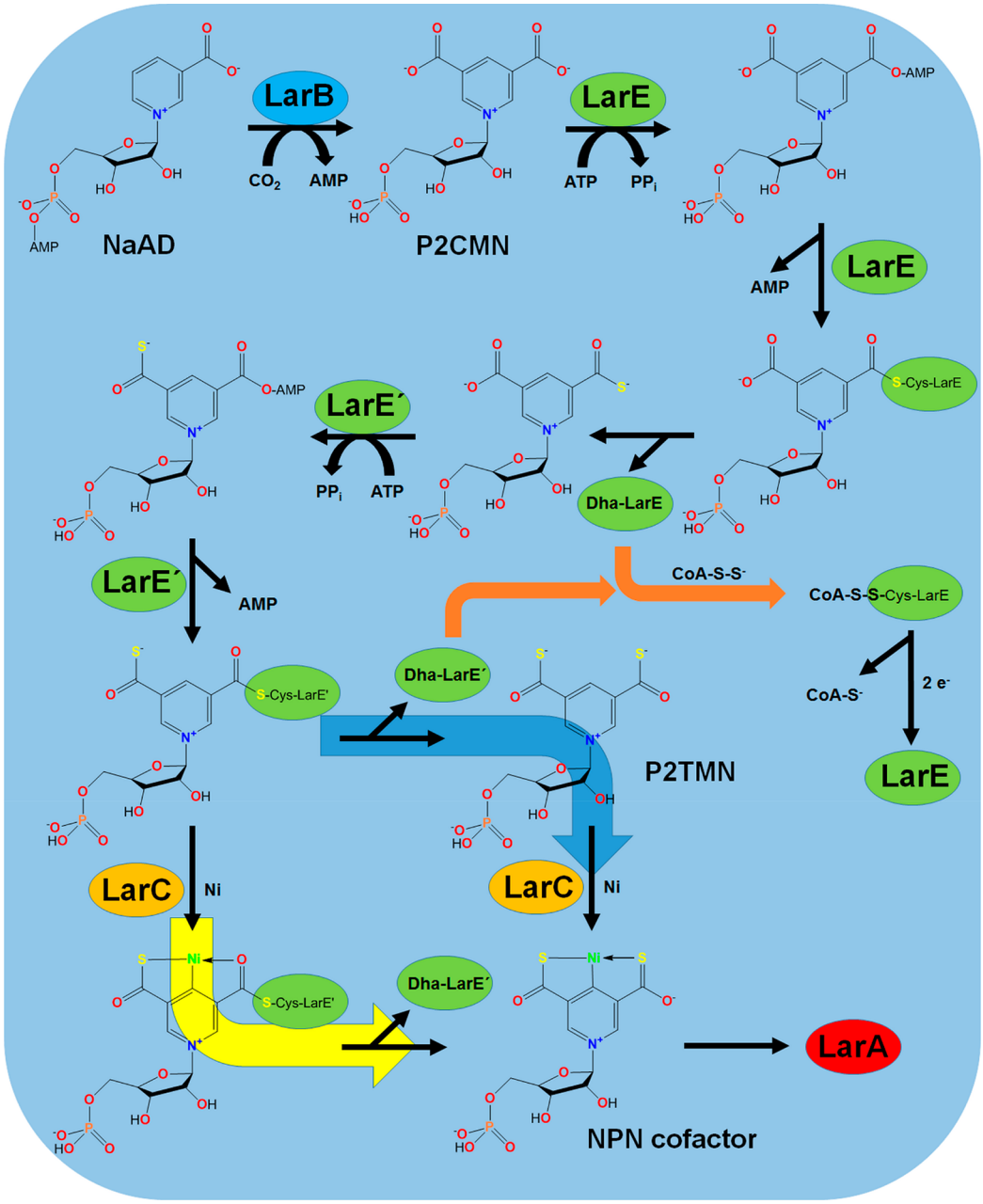

Figure 8. Biosynthesis of the NPN cofactor for LarA apoprotein activation, regeneration of LarE^{Dha}, and an alternate pathway to generate lactate racemase activity. In the predominant pathway, LarB carboxylates nicotinic acid adenine dinucleotide (NaAD) and hydrolyzes its phosphoanhydride linkage, thus forming P2CMN. LarE activates the substrate carboxyl group by adenylylation, forms a thioester linkage with the substrate, and sacrifices its Cys176 sulfur atom, and then a second LarE repeats the cycle to produce P2TMN (blue arrow). LarC inserts nickel into this species to generate the NPN cofactor that activates LarA. LarE^{Dha} can be regenerated to native LarE by incubation with CoA persulfide and reductant (orange arrows), but it is unclear whether these reactions are physiologically relevant. A newly identified NPN-LarE intermediate functions in an alternative, minor pathway (yellow arrow) in which LarC installs nickel into the pincer cofactor while it is still bound to LarE. NPN is released from this purified protein for LarA activation.

of the substrate, P2CMN. Furthermore, Glu223 forms hydrogen bonds to the nearby Arg214 and Arg221 residues, with Arg214 being directly involved in phosphate binding. The E223A variant exhibited no significant change in activity compared to the WT enzyme. This finding shows that the interaction of Arg214 with phosphate is unlikely to require Glu223 so that phosphate binding requires only Ser180 and Arg212 (Figure 7B). The Arg214/Glu223 interaction is structurally similar to the nearby Arg181/Glu200 interaction, but in that case, the E200Q variant was inactive, highlighting the importance of the Glu200 side chain. Second, we examined Lys101 that is conserved in LarE sequences and forms a salt bridge with AMP (Figure 7B). Surprisingly, the K101A variant was as active as the WT enzyme, suggesting that the lysine is not critical for stabilizing AMP binding and that other residues on a nearby flexible loop might compensate for its absence through other AMP phosphate interaction residues.[9] Asp128 is another highly conserved residue on the flexible loop, but this residue does not directly interact with AMP in the crystal structure (Figure 7B). At a distance of 6.2 Å from the AMP

DOI: 10.1021/acs.biochem.8b00601
Biochemistry 2018, 57, 5513−5523

phosphate, it is unclear what role this residue could play; nevertheless, it must be important as the D128A variant was inactive. This result demonstrates a key role for the flexible loop containing Asp128, either in its disordered state found in most structures or as the helical fold in the AMP-bound structure.

DISCUSSION

NPN Biosynthesis, LarE^{Dha} Regeneration, and a New Pathway for LarA Activation. We combine our new results with those from prior studies in a summary depiction of the LarA apoprotein activation process (Figure 8). In the primary pathway, LarB converts NaAD to P2CMN,[8] two molecules of LarE catalyze AMPylation of the pyridinium carboxyl groups followed by sacrificial sulfur transfers from Cys176 to form P2TMN (generating two copies of LarE^{Dha}),[8,9] LarC inserts nickel by a CTP-dependent process,[8,10] and the resulting free NPN activates LarA (Figure 8, blue arrow pathway).

We have now shown that LarE^{Dha} can be recycled to regenerate native LarE by *in vitro* incubation with CoA persulfide and reductant (Scheme 1 and Figure 8, orange arrows). The CoA persulfide is likely to bind at the CoA binding site of LarE for this reaction because other tested persulfides were inefficient or not effective. Such binding would perfectly position the persulfide to react with Dha. Persulfides are known to have increased nucleophilic character compared to thiols and are of increasing interest in biology.[23,24] CoA persulfide is found in cells[25,26] and has been shown to bind tightly to short chain acyl-CoA dehydrogenases.[27,28] Although CoA persulfide is an attractive candidate for recycling LarE^{Dha}, the near exclusive presence of this form of the protein in *Lc. lactis* cells containing pGIR172 suggests this reaction is not physiologically relevant and LarE is a single-turnover enzyme.

Our finding of what appears to be an NPN-LarE adduct suggests that LarC can insert nickel into the incomplete pincer ligand that is still bound in the thioester linkage to LarE (Figure 8, yellow arrow). The flexibility of the LarE loop containing Cys176 could reasonably allow the pincer species to be metalated by LarC. The NPN-LarE species is presumed to release NPN, accounting for the previously reported activation of LarA apoprotein by just LarE,[5] resulting in the generation of the LarE^{Dha} form of the protein. The *in vivo* relevance of the NPN-LarE adduct remains to be clarified; this species may be abundant within the cell but converts to LarE^{Dha} as the protein is purified.

LarE Homologues: Potential Roles of Additional Cysteine Residues. We had previously noted that many LarE homologues have sequences in which Cys176 appears to be shifted by one residue and points toward two additional cysteine residues, not present in the *L. plantarum* LarE sequence, one of which substitutes for Trp97 (Figure 9A,B).[9] We speculate that these alternative LarE versions might catalyze a different mechanism of sulfur transfer that does not require sacrifice of a side chain sulfur atom as observed in the benchmark LarE. Comparison of the location for these cysteine residues in a model of *T. thermosaccharolyticum* LarE (Figure 9B)[9] to the structure of *Thermus thermophilus* TtuA,[29] another PP-loop pyrophosphatase family member that catalyzes sulfur transfer for 2-thiouridine synthesis, reveals the similarity of the LarE ortholog and the [4Fe-4S] cluster binding site bound by three cysteine residues in TtuA (Figure 9C). In that case, the sulfur transferred to uridine is suggested to derive from the non-[4Fe-4S] cluster sulfide atom (positioned where a fourth cysteine is found for many similar clusters), which must be replaced for each round of synthesis.[29] Structural similarities and sulfur transfer involving a labile extra cluster sulfide were noted in a study of TtuA from *Pyrococcus horikoshii* that also possesses a [4Fe-4S] cluster bound by three cysteines (Figure 9D).[30] Furthermore, the structure of the more distantly related ortholog adenosine 5′-phosphosulfate reductase from *Pseudomonas aeruginosa* also reveals a [4Fe-4S] cluster at this site;[31] however, in that case, four protein cysteine residues are present and the cluster is not thought to donate a sulfur atom (Figure 9E). Rather, this enzyme uses its [4Fe-4S] and flavin to reversibly transfer electrons from sulfite and AMP while forming adenylyl sulfate and a reduced electron acceptor. Interestingly, two other structurally related sulfur transferases, tRNA 2-thiouridylase or MnmA from *E. coli* (Figure 9F)[32] and tRNA 4-thiouridine synthetase or ThiI from *Thermotoga maritima* (Figure 9G),[33] also contain their catalytic cysteine residues in the same region as LarE's Cys176. In these cases, cysteine persulfides are generated, with disulfide exchange involving another cysteine residue allowing for the insertion of a sulfur atom into the substrate. Although the structure has not been obtained, ThiI from *Methanococcus maripaludis* was shown to possess a [3Fe-4S] cluster that was needed for sulfur transfer.[34]

One precedent exists for a sacrificial sulfur transferase, THI4p that functions in the thiamine biosynthesis pathway of

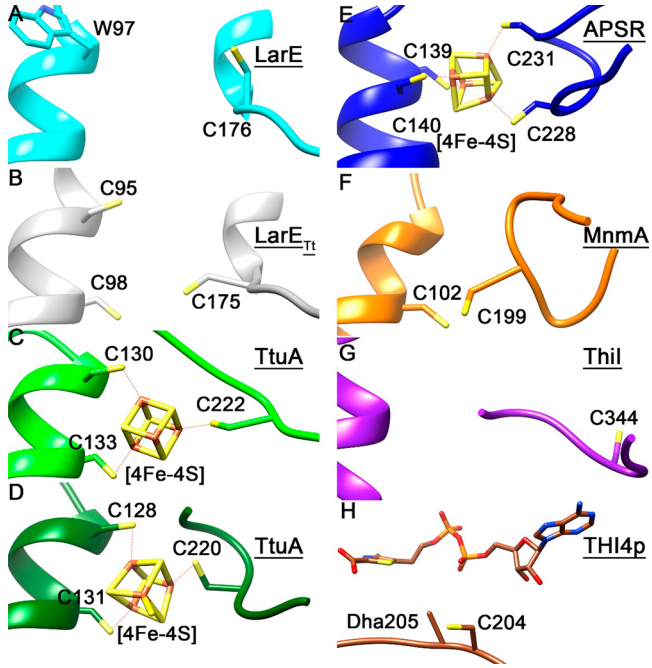

Figure 9. Comparison of active sites of structurally related sulfur transferases. (A) LarE from *L. plantarum* colored cyan (PDB entry 5UDR). (B) Homology model of LarE$_{Tt}$ from *T. thermosaccharolyticum* colored gray. (C) 2-Thiouridine synthetase (TtuA) from *Th. thermophilus* colored light green (PDB entry 5B4E). (D) TtuA from *P. horikoshii* colored dark green (PDB entry 5MKP). (E) Adenosine 5′-phosphosulfate reductase from *Ps. aeruginosa* colored blue (PDB entry 2GOY). (F) tRNA 2-thiouridylase (MnmA) from *E. coli* colored orange (PDB entry 2DEU). (G) tRNA 4-thiouridine synthetase (ThiI) from *Thm. maritima* colored purple (PDB entry 4KR6). (H) Functionally related sacrificial sulfur insertase (THI4p) from *S. cerevisiae* colored brown with bound adenylylated thiazole (PDB entry 3FPZ).

DOI: 10.1021/acs.biochem.8b00601
Biochemistry 2018, 57, 5513−5523

Saccharomyces cerevisiae.[35] Although related in function to LarE and similarly thought to catalyze a single turnover, THI4p possesses a distinct fold (Figure 9H). Of further interest, *Methanococcus jannaschii* possesses an ortholog of THI4p that uses exogenous sulfide for thiamin biosynthesis and is catalytic.[36] This example, like that mentioned above for ThiI, illustrates the situation in which orthologs of the same protein can exhibit distinct properties. In this case, one example is a sacrificial single-turnover enzyme while the other ortholog exhibits multiple-turnover catalytic activity.

LarE is structurally related to other sulfur transferases that contain [4Fe-4S] clusters or generate persulfides at their active sites, such as TtuA, MnmA, and ThiI. In addition, it is functionally related to sulfur transfer enzymes in thiamin synthesis that utilize two distinct mechanisms, one stoichiometric and one catalytic. Thus, we hypothesize that other LarE orthologs may bind a [4Fe-4S] cluster or generate persulfides and use these species for catalytic sulfur transfer. LarE homologues that use three active site cysteine residues to bind a [4Fe-4S] cluster could use the nonligated sulfur atom for attack of the AMPylated substrate without sacrificing a cysteine residue. Similarly, a persulfide could attack the adenylylated substrate with another cysteine forming a disulfide to allow for sulfur transfer. The active form of the enzyme could then be reconstituted by the normal cellular cluster synthesis machinery or by persulfide formation to allow for additional rounds of sulfur transfer. It will be interesting to assess whether LarE functions catalytically in the multi-Cys proteins.

CONCLUSIONS

We elucidated the structure of the complex between CoA and LarE and unexpectedly observed strong similarities in binding modes for CoA and ATP. The sulfur atom of CoA can adopt multiple positions, including formation of the previously identified disulfide with Cys176 of LarE, and the structures provide insights into how CoA provides thermal stability to the protein. The persulfide of CoA was competent for restoring the sulfur atom to LarE^{Dha}, whereas other LarE regeneration efforts were poorly effective or unsuccessful. The low extent of LarE recycling *in vitro* and the lack of evidence for *in vivo* recycling are consistent with our prior conclusion that LarE is a sacrificial protein.[9] Only two LarE molecules are required for activation of each cofactor that becomes bound to LarA, so a stoichiometric mechanism may be sufficient for cellular needs. We identified a new species, the NPN adduct of LarE that explains the perplexing prior results in which purified LarE was sufficient to activate LarA apoprotein. Release of NPN from the small proportion of LarE with a bound cofactor accounted for LarA activation when using a vast excess of the accessory protein. The observation of this adduct shows that LarC can catalyze the metalation reaction of the organic ligand bound in a thioester linkage to LarE. We determined the structure of the C176A variant and found that the lack of the thiol side chain led to no conformational changes compared to the conformation of the WT enzyme. We also created three additional active site variants of LarE and discussed their activities in a structural context, along with those of previously described variants. Finally, we performed a structural comparison of the *L. plantarum* LarE to a homology model for an alternative version of LarE with a predicted cluster of cysteine residues and other related enzymes that possess [4Fe-4S] clusters or a reactive persulfide in their active sites. From this analysis, we speculate that some orthologs of LarE may bind a [4Fe-4S] cluster providing them with the ability to act catalytically. Our supposition of two forms of an enzyme, one acting stoichiometrically to form LarE^{Dha} and the other acting catalytically, has precedence in thiamin biosynthesis.

ASSOCIATED CONTENT

Supporting Information

The Supporting Information is available free of charge on the ACS Publications website at DOI: 10.1021/acs.biochem.8b00601.

Mass spectrometric results for the interaction of TCEP, CoA, and DTT with LarE^{Dha} (Figures S1−S3, respectively) (PDF)

AUTHOR INFORMATION

Corresponding Author

*E-mail: hausinge@msu.edu.

ORCID

Matthias Fellner: 0000-0003-3192-6984
Joel A. Rankin: 0000-0002-9775-4508
Benoît Desguin: 0000-0002-5004-6918
Jian Hu: 0000-0001-6657-9826
Robert P. Hausinger: 0000-0002-3643-2054

Present Address

⊥M.F.: Department of Biochemistry, University of Otago, P.O. Box 56, Dunedin 9054, New Zealand.

Author Contributions

M.F. and J.A.R. contributed equally to this work.

Funding

This work was supported by the National Science Foundation (Grants CHE-1516126 and CHE-1807073 to R.P.H. and J.H.).

Notes

The authors declare no competing financial interest.

ACKNOWLEDGMENTS

The authors thank Tony Schilmiller of the Michigan State University Mass Spectrometry Core Facility for advice and Eugene Mueller (University of Louisville, Louisville, KY) for providing pBH402 encoding IscS.

REFERENCES

(1) Juturu, V., and Wu, J. C. (2016) Microbial production of lactic acid: The latest development. *Crit. Rev. Biotechnol. 36*, 967−977.

(2) Desguin, B., Soumillion, P., Hols, P., Hu, J., and Hausinger, R. P. (2017) Lactate racemase and its niacin-derived, covalently-tethered, nickel cofactor. In *Biological Chemistry of Nickel* (Zamble, D., Rowinska-Zyrek, and Kozlowski, H., Eds.) pp 220−236, Royal Society of Chemistry.

(3) Fellner, M., Rankin, J. A., Hu, J., and Hausinger, R. P. (2017) Lactate racemase. In *Encyclopedia of Inorganic and Bioinorganic Chemistry*, John Wiley & Sons, Ltd.

(4) Desguin, B., Soumillion, P., Hausinger, R. P., and Hols, P. (2017) Unexpected complexity in the lactate racemization system of lactic acid bacteria. *FEMS Microbiol. Rev. 41*, S71−S83.

(5) Desguin, B., Goffin, P., Viaene, E., Kleerebezem, M., Martin-Diaconescu, V., Maroney, M. J., Declercq, J. P., Soumillion, P., and Hols, P. (2014) Lactate racemase is a nickel-dependent enzyme activated by a widespread maturation system. *Nat. Commun. 5*, 3615.

DOI: 10.1021/acs.biochem.8b00601
Biochemistry 2018, 57, 5513−5523

(6) Desguin, B., Zhang, T., Soumillion, P., Hols, P., Hu, J., and Hausinger, R. P. (2015) A tethered niacin-derived pincer complex with a nickel-carbon bond in lactate racemase. *Science 349*, 66−69.
(7) Hausinger, R. P., Desguin, B., Fellner, M., Rankin, J. A., and Hu, J. (2018) Nickel pincer nucleotide cofactor. *Curr. Opin. Chem. Biol. 47*, 18−23.
(8) Desguin, B., Soumillion, P., Hols, P., and Hausinger, R. P. (2016) Nickel-pincer cofactor biosynthesis involves LarB-catalyzed pyridinium carboxylation and LarE-dependent sacrificial sulfur insertion. *Proc. Natl. Acad. Sci. U. S. A. 113*, 5598−5603.
(9) Fellner, M., Desguin, B., Hausinger, R. P., and Hu, J. (2017) Structural insights into the catalytic mechanism of a sacrificial sulfur insertase of the N-type ATP pyrophosphatase family, LarE. *Proc. Natl. Acad. Sci. U. S. A. 114*, 9074−9079.
(10) Desguin, B., Fellner, M., Riant, O., Hu, J., Hausinger, R. P., Hols, P., and Soumillion, P. (2018) Biosynthesis of the nickel-pincer nucleotide cofactor of lactate racemase requires a CTP-dependent cyclometallase. *J. Biol. Chem. 293*, 12303.
(11) Krug, M., Weiss, M. S., Heinemann, U., and Mueller, U. (2012) XDSAPP: a graphical user interface for the convenient processing of diffraction data using XDS. *J. Appl. Crystallogr. 45*, 568−572.
(12) Battye, T. G., Kontogiannis, L., Johnson, O., Powell, H. R., and Leslie, A. G. (2011) iMOSFLM: a new graphical interface for diffraction-image processing with MOSFLM. *Acta Crystallogr., Sect. D: Biol. Crystallogr. 67*, 271−281.
(13) Evans, P. R., and Murshudov, G. N. (2013) How good are my data and what is the resolution? *Acta Crystallogr., Sect. D: Biol. Crystallogr. 69*, 1204−1214.
(14) Adams, P. D., Afonine, P. V., Bunkoczi, G., Chen, V. B., Davis, I. W., Echols, N., Headd, J. J., Hung, L. W., Kapral, G. J., Grosse-Kunstleve, R. W., McCoy, A. J., Moriarty, N. W., Oeffner, R., Read, R. J., Richardson, D. C., Richardson, J. S., Terwilliger, T. C., and Zwart, P. H. (2010) PHENIX: a comprehensive Python-based system for macromolecular structure solution. *Acta Crystallogr., Sect. D: Biol. Crystallogr. 66*, 213−221.
(15) Emsley, P., Lohkamp, B., Scott, W. G., and Cowtan, K. (2010) Features and development of Coot. *Acta Crystallogr., Sect. D: Biol. Crystallogr. 66*, 486−501.
(16) Pettersen, E. F., Goddard, T. D., Huang, C. C., Couch, G. S., Greenblatt, D. M., Meng, E. C., and Ferrin, T. E. (2004) UCSF Chimera–a visualization system for exploratory research and analysis. *J. Comput. Chem. 25*, 1605−1612.
(17) Riddles, P. W., Blakeley, R. L., and Zerner, B. (1979) Ellman's reagent: 5,5′-dithiobis(2-nitrobenzoic acid) – a reexamination. *Anal. Biochem. 94*, 75−81.
(18) Scian, M., Guttman, M., Bouldin, S. D., Outten, C. E., and Atkins, W. M. (2016) The myeloablative drug busulfan converts cysteine to dehydroalanine and lanthionine in redoxins. *Biochemistry 55*, 4720−4730.
(19) Englander, S. W., Calhoun, D. B., and Englander, J. J. (1987) Biochemistry without oxygen. *Anal. Biochem. 161*, 300−306.
(20) Mueller, E. G., Palenchar, P. M., and Buck, C. J. (2001) The role of the cysteine residues of ThiI in the generation of 4-thiouridine in tRNA. *J. Biol. Chem. 276*, 33588−33595.
(21) Kabil, O., and Banerjee, R. (2012) Characterization of patient mutations in human persulfide dioxygenase (ETHE1) involved in H_2S catabolism. *J. Biol. Chem. 287*, 44561−44567.
(22) Wood, J. L. (1987) Sulfane sulfur. *Methods Enzymol. 143*, 25−29.
(23) Cuevasanta, E., Möller, M. N., and Alvarez, B. (2017) Biological chemistry of hydrogen sulfide and persulfides. *Arch. Biochem. Biophys. 617*, 9−25.
(24) Park, C.-M., Weerasinghe, L., Day, J. J., Fukuto, J. M., and Xian, M. (2015) Persulfides: Current knowledge and challenges in chemistry and chemical biology. *Mol. BioSyst. 11*, 1775−1785.
(25) Shen, J., Keithly, M. E., Armstrong, R. N., Higgins, K. A., Edmonds, K. A., and Giedroc, D. P. (2015) *Staphylococcus aureus* CstB is a novel multidomain persulfide dioxygenase-sulfurtransferase involving in hydrogen sulfide deteoxification. *Biochemistry 54*, 4542−4554.
(26) Shen, J., Walsh, B. J. C., Flores-Mireles, A. L., Peng, H., Zhang, Y., Zhang, Y., Trinidad, J. C., Hultgren, S. J., and Giedroc, D. P. (2018) Hydrogen sulfide sensing through reactive sulfur species (RSS) and nitroxyl (HNO) in *Enterococcus faecalis*. *ACS Chem. Biol. 13*, 1610−1626.
(27) Shaw, L., and Engel, P. C. (1987) CoA-persulfide: a possible in vivo inhibitor of mammalian short-chain acyl-CoA dehydrogenase. *Biochim. Biophys. Acta, Lipids Lipid Metab. 919*, 171−174.
(28) Tiffany, K. A., Roberts, D. L., Wang, M., Paschke, R., Mohsen, A.-W. A., Vockley, J., and Kim, J.-J. P. (1997) Structure of human isovaleryl-CoA dehydrogenase at 2.6 Å resolution: Structural basis for substrate specificity. *Biochemistry 36*, 8455−8464.
(29) Chen, M., Asai, S. I., Narai, S., Nambu, S., Omura, N., Sakaguchi, Y., Suzuki, T., Ikeda-Saito, M., Watanabe, K., Yao, M., Shigi, N., and Tanaka, Y. (2017) Biochemical and structural characterization of oxygen-sensitive 2-thiouridine synthesis catalyzed by an iron-sulfur protein TtuA. *Proc. Natl. Acad. Sci. U. S. A. 114*, 4954−4959.
(30) Arragain, S., Bimai, O., Legrand, P., Caillat, S., Ravanat, J. L., Touati, N., Binet, L., Atta, M., Fontecave, M., and Golinelli-Pimpaneau, B. (2017) Nonredox thiolation in tRNA occurring via sulfur activation by a [4Fe-4S] cluster. *Proc. Natl. Acad. Sci. U. S. A. 114*, 7355−7360.
(31) Chartron, J., Carroll, K. S., Shiau, C., Gao, H., Leary, J. A., Bertozzi, C. R., and Stout, C. D. (2006) Substrate recognition, protein dynamics, and iron-sulfur cluster in *Pseudomonas aeruginosa* adenosine 5′-phosphosulfate reductase. *J. Mol. Biol. 364*, 152−169.
(32) Numata, T., Ikeuchi, Y., Fukai, S., Suzuki, T., and Nureki, O. (2006) Snapshots of tRNA sulphuration via an adenylated intermediate. *Nature 442*, 419−424.
(33) Neumann, P., Lakomek, K., Naumann, P. T., Erwin, W. M., Lauhon, C. T., and Ficner, R. (2014) Crystal structure of a 4-thiouridine synthetase-RNA complex reveals specificity of tRNA U8 modification. *Nucleic Acids Res. 42*, 6673−6685.
(34) Liu, Y., Vinyard, D. J., Reesbeck, M. E., Suzuki, T., Manakongtreecheep, K., Holland, P. L., Brudvig, G. W., and Soll, D. (2016) A [3Fe-4S] cluster is required for tRNA thiolation in archaea and eukaryotes. *Proc. Natl. Acad. Sci. U. S. A. 113*, 12703−12708.
(35) Chatterjee, A., Abeydeera, N. D., Bale, S., Pai, P. J., Dorrestein, P. C., Russell, D. H., Ealick, S. E., and Begley, T. P. (2011) *Saccharomyces cerevisiae* THI4p is a suicide thiamine thiazole synthase. *Nature 478*, 542−546.
(36) Eser, B. E., Zhang, X., Chanani, P. K., Begley, T. P., and Ealick, S. E. (2016) From suicide enzyme to catalyst: The iron-dependent sulfide transfer in *Methanococcus jannaschii* thiamin thiazole biosynthesis. *J. Am. Chem. Soc. 138*, 3639−3642.

DOI: 10.1021/acs.biochem.8b00601
Biochemistry 2018, 57, 5513−5523